Induction of Autoimmunity in a Bleomycin-Induced Murine Model of Experimental Systemic Sclerosis: An Important Role for CD4$^+$ T Cells

Hideaki Ishikawa[1,3], Kozue Takeda[1], Akira Okamoto[2], Sei-ichi Matsuo[3] and Ken-ichi Isobe[1]

Systemic sclerosis (SSc) is an autoimmune disease characterized by the excessive deposition of collagen in the skin or other organs and the production of specific antinuclear antibodies (ANAs). Recently, bleomycin (BLM)-induced experimental scleroderma was reported in a murine model. Here, we present further development of this model and suggest that it is appropriate for the analysis of human diffuse type SSc. BLM was injected into the shaved backs of C3H or BALB/c mice (100 μg/mouse) 5 days per week for 3 weeks. Skin fibrosis was confirmed and pathological changes were seen in the lower part of the esophagus and stomach similar to those seen in SSc. The sera from these mice had autoantibodies specific to the damaged tissues and ANAs. Transfer of CD4$^+$ T cells from BLM-treated BALB/c mice induced the same pathological changes and antibody production in untreated-BALB/c nude mice. Hence, tissue fibrosis and the production of ANAs are probably associated with CD4$^+$ T-cell activity in this model. In conclusion, this model will be valuable for investigating the relationship between tissue fibrosis and abnormalities of the immune system.

Journal of Investigative Dermatology (2009) **129,** 1688–1695; doi:10.1038/jid.2008.431; published online 22 January 2009

INTRODUCTION

Systemic sclerosis (SSc) is an autoimmune disease of connective tissue that is highly heterogeneous in its clinical manifestations (Abraham and Varga, 2005; Varga and Abraham, 2007). Although family and twin studies suggest that a genetic component is important (Arnett *et al.*, 2001), several environmental factors are believed to be causative (Nietert and Silver, 2000). There is no established therapy for SSc. Animal models are needed to reveal the precise mechanisms of fibrosis and autoimmunity in SSc. Bleomycin (BLM) is a copper-chelating peptide that can cleave DNA, and it is widely used as an anti-tumor agent for various types of malignancies, including squamous cell carcinomas and lymphoma (Hay *et al.*, 1991; Povirk and Austin, 1991; Tokuhashi *et al.*, 1997; Burger, 1998). BLM-induced tissue injury has been extensively studied in a BLM-induced model of pulmonary fibrosis (Bowden, 1984). Intra-dermal administration of BLM in mice has been shown to induce skin fibrosis that closely resembles SSc (Yamamoto *et al.*, 1999; Lakos *et al.*, 2006; Yamamoto, 2006). Autoantibody production was also detectable in this model (Yamamoto *et al.*, 1999), indicating that BLM treatment induces autoimmunity. Evidence of autoimmunity has not been described in previous reports. In this study, we evaluated the pathogenesis of BLM-induced autoimmunity and determine the potential utility of this system as a model of human SSc.

[1]*Department of Immunology, Nagoya University Graduate School of Medicine, Nagoya, Aichi, Japan;* [2]*Department of Molecular Bacteriology, Nagoya University Graduate School of Medicine, Nagoya, Aichi, Japan and* [3]*Department of Nephrology, Nagoya University Graduate School of Medicine, Nagoya, Aichi, Japan*

Correspondence: Dr Ken-ichi Isobe, Department of Immunology, Nagoya University Graduate School of Medicine, 65 Tsurumai-cho, Showa-ku, Nagoya, Aichi 466-8550, Japan. E-mail: kisobe@med.nagoya-u.ac.jp

Abbreviations: Ab, antibody; ANA, antinuclear antibody; BLM, bleomycin; MaT, Masson's trichrome; PBS, phosphate-buffered saline; SSc, systemic sclerosis

Received 29 July 2008; revised 29 October 2008; accepted 25 November 2008; published online 22 January 2009

RESULTS

Pathological and clinical manifestation of this model

At the site of BLM injection, we found an increase in skin thickness, a decrease in the amount of subcutaneous fat tissue, and robust deposition of collagen as determined by Masson's trichrome (MaT) (Figure 1a–e). These were the same histopathological features previously reported for fibrosis (Yamamoto *et al.*, 1999). Surprisingly, we found BLM-induced damage at other sites (Figure 1a–e). It can be noted that, the lower part of the esophagus was affected. We detected a diminished esophageal wall due to atrophy of the smooth muscle (Figure 1a–e). In MaT staining of the esophagus, smooth muscle was stained blue, suggesting that atrophy of the esophageal smooth muscle was correlated with fibrosis (Figure 1a–e). We also detected tissue damage in the stomach where shrinkage of the submucosal layer was seen (Figure 1a–e). The submucosal layer was rendered blue by MaT staining (data not shown); hence, this pathological change was also fibrotic. These tissue changes were measured and found to be statistically significant (Figure 1c–e). When the tissue damage found in the dermis of the skin was compared with that of the esophagus and stomach, we detected some

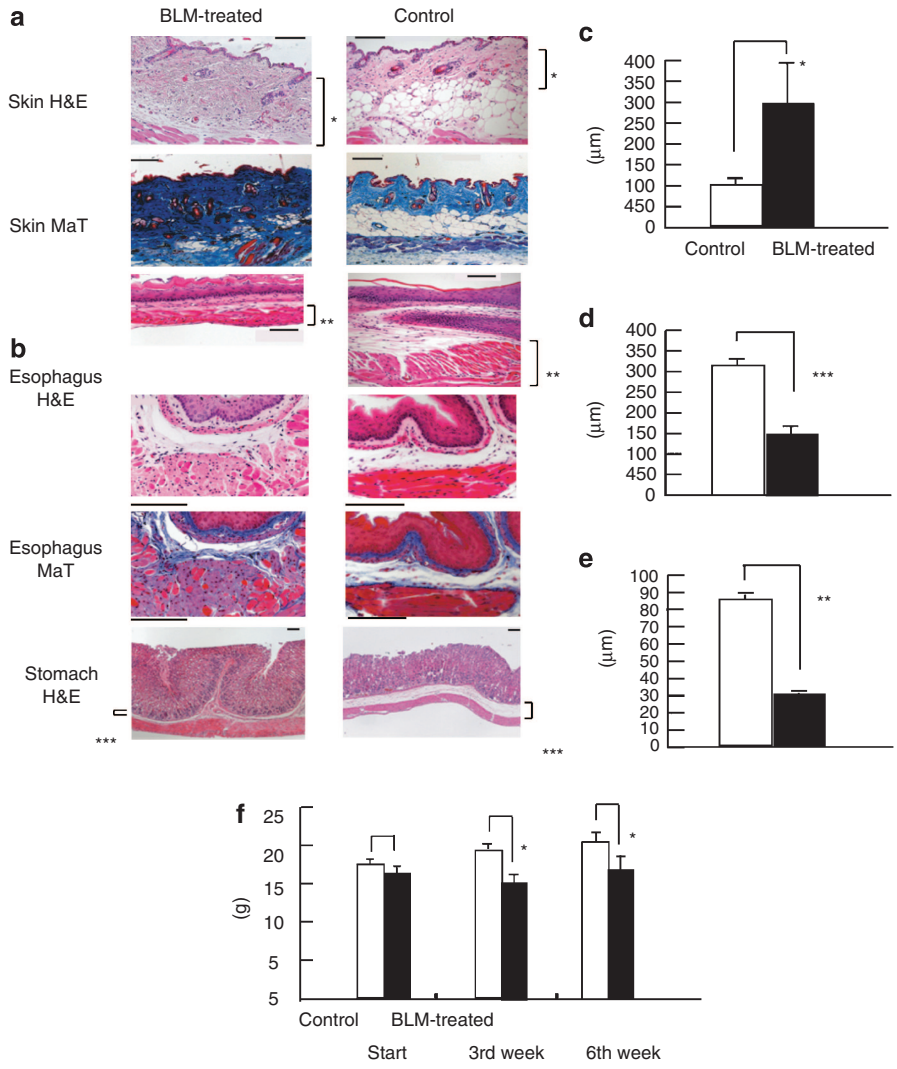

Figure 1. Pathogenesis associated with fibrosis in BLM-treated mice. C3H mice were injected subcutaneously with PBS, or 100 μg of BLM (see Materials and Methods). Representative tissue changes for C3H mice are shown (**a**–**e**). (**a**) Skin H&E and skin MaT, where * indicates dermis of the skin. (**b**) Esophagus H&E: long axis, esophagus: short axis, where ** indicates smooth muscle layer of the esophagus. Esophagus MaT: short axis. Fibrotic changes in smooth muscle were observed. Stomach H&E, where *** indicates submucosal layer of the stomach. Bars = 100 μm. Comparison of (**c**) the dermis, $*P<0.05$; (**d**) smooth muscle layer, $***P<0.001$; and (**e**) submucosal layer, $**P<0.01$. Representative comparison data were shown in panels a–e. (**f**) Time course of body weight changes in this model. Data are means ± SD (control, $n=10$; BLM-treated, $n=10$). Body weight loss was observed and it continued even 3 weeks after BLM treatment. $*P<0.05$.

interesting differences. In the skin, increased deposition of collagen fibers was the primary result. In contrast, in the esophagus and stomach, fibrosis of the smooth muscle itself or the submucosal layer was observed. In both cases, these pathological changes were likely associated with fibrosis. Fibrosis around a small artery and the interstitium of the kidney was also observed (data not shown). No apparent fibrosis in the lung, heart, liver, and small intestine was observed in C3H mice (data not shown). We also investigated tissue damage 3 weeks after the termination of BLM treatment. Interestingly, tissue damage was still observed (data not shown).

We further evaluated tissue fibrosis by α-smooth muscle actin staining (see Figure S1). We also compared the body weights of these two groups. At the conclusion of BLM treatment, the body weights of the BLM-treated mice were significantly decreased (Figure 1f). Cytotoxic effects of BLM may contribute to the loss of body weights, perhaps associated with the gastric damage shown in Figure 1e.

Autoantibodies and antinuclear antibody production in this model

Specific antibodies (Abs), particularly antinuclear antibody (ANA), are involved in the pathogenesis of human SSc. We detected the ANA with NIH3T3 and Hep2 targets using sera from BLM-treated subjects. We concluded that the staining pattern was anti-nucleolar (Figure 2a–d). Thus, sera from BLM-treated animals contained ANA, which react with both murine and human antigens.

Using sera from BLM-treated mice in western blots, several bands were detected against every tissue examined (Figure 3a). Immunofluorescence was also performed on a stomach section taken from a control mouse (Figure 3b and c). This result suggests that an autoantibody directed against the gastric mucosa was present in BLM-treated mice. This result supports immunoblot data using stomach extracts (Figure 3a–c). Taken together, we confirmed the extended production of autoantibodies (including ANAs) after BLM administration (Figures 2 and 3). These data suggest that autoantibodies production and gastrointestinal deterioration reflect BLM-mediated pathogenesis in this model of SSc.

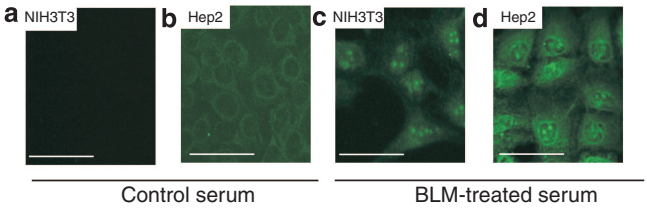

Figure 2. Antinuclear antibodies produced in the model. (**a**–**d**) ANAs were detected using NIH3T3 and Hep2 targets. The staining pattern in Hep2 is recognizable as an antinucleolar pattern (**b** and **d**). Bars = 50 μm. Data are representative of three separate experiments.

BLM treatment damaged CD4$^+$ T cells

To investigate immune reactions in this model, we examined the thymus and spleen at different times during and after treatment. Apparent cytopenia of the thymus and spleen was observed after BLM administration (Figure 4a–k). Interestingly, in both the thymus and spleen, the number of CD4$^+$ T cells was significantly decreased, possibly due to cytotoxic effect of BLM. The size of the thymus was obviously decreased in the BLM-treated group (Figure 4e). Pathological analysis showed the destruction of the thymic cortex in

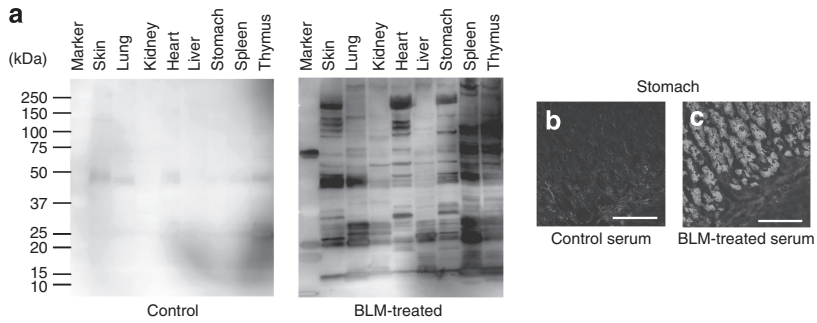

Figure 3. Autoantibodies in sera from BLM-treated mice. (**a**) Tissue antigens detected by western blotting. Serum samples (10 μl) were taken the day following the final BLM treatment (day 22), six mice per group. Protein samples were prepared as described in Materials and Methods. (**b** and **c**) Antibodies to normal stomach were detected. Bar = 100 μm. Representative data from several independent experiments are shown.

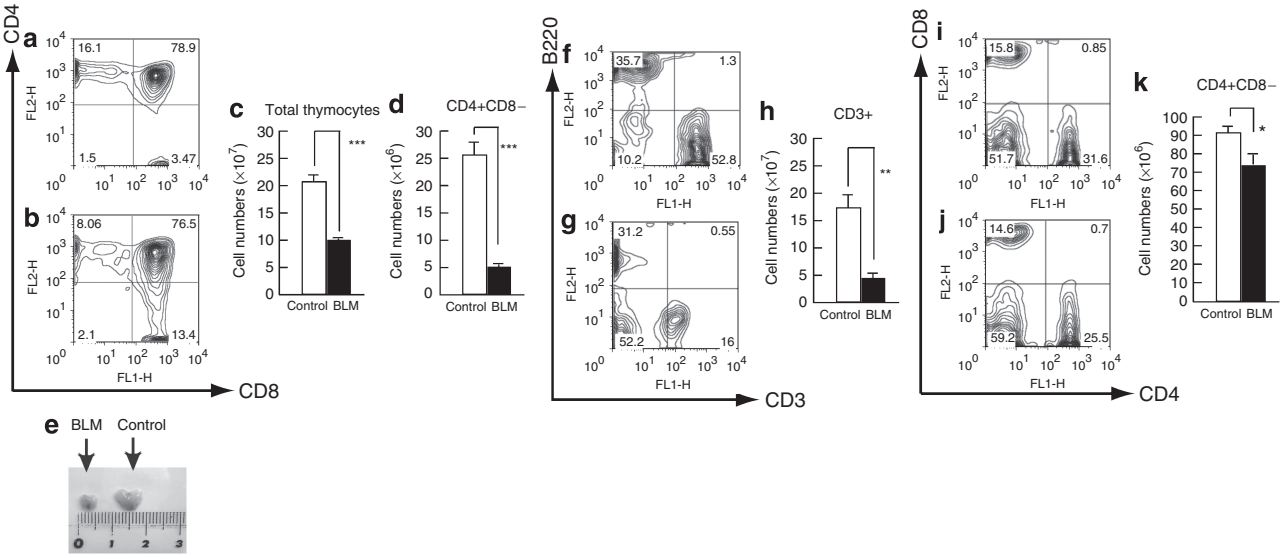

Figure 4. BLM-induced damage to the thymus and spleen. (**a**–**e**) Significant decrease in CD4$^+$ T cells in the thymus. Thymus from (**a**) control and (**b**) BLM-treated mice. (**c**) Comparison of total thymocytes. (**d**) Comparison of CD4$^+$CD8$^-$ cells. Data are means ± SD (control, $n = 4$; BLM-treated, $n = 4$). Representative of three separate experiments. (**e**) Atrophy of the thymus in BLM-treated mice. (**f**–**j**) Significant decrease in CD4$^+$ T cells in the spleen. Splenocytes from (**f**, **i**) control, and (**g**, **j**) BLM-treated mice. (**h**) Comparison of CD3$^+$ cells. (**k**) Comparison of CD4$^+$CD8$^-$ cells. Data are means ± SD (control, $n = 4$; BLM-treated, $n = 4$). *$P < 0.05$; **$P < 0.01$; and ***$P < 0.001$. Representative of three separate experiments.

BLM-treated mice (data not shown). This result suggests that BLM might have inhibited $CD4^+$ T cells' maturation. In the spleen, the total number of T cells was significantly reduced due to decreasing numbers of $CD4^+$ T cells (Figure 4f–k). Taken together, these data suggested that $CD4^+$ T cells are particularly susceptible to the effects of BLM in both the thymus and spleen. The sensitivity of $CD4^+$ T cells may be associated with the induction of autoimmunity in this model.

Adaptive cell transfer of BLM-treated lymphocytes reproduce tissue fibrosis

Our results (Figures 2 and 3) suggest the presence of an autoimmune response in BLM-treated mice. We postulated that splenocytes of BLM-treated mice included a population of autoimmune T cells, and therefore the adaptive cell transfer was performed. The experimental design for this experiment is described in the Materials and Methods section. We observed increased collagen fibers in the dermis of the skin in BALB/c and C3H mice. Hypertrophy of the gastric mucosa was also induced in BLM-treated BALB/c mice (Figure 5a and b). Interestingly, nearly the same tissue changes were present in the recipient mice and BLM-treated donors (Figure 5c and d). No tissue changes were found in control donor mice (Figure 5e and f; PBS-treated BALB/c mice), and no tissue changes were induced in the recipient mice (Figure 5g and h). Taken together, we confirmed that skin fibrosis and fibrotic gastritis were directly induced by BLM-induced autoreactive lymphocytes.

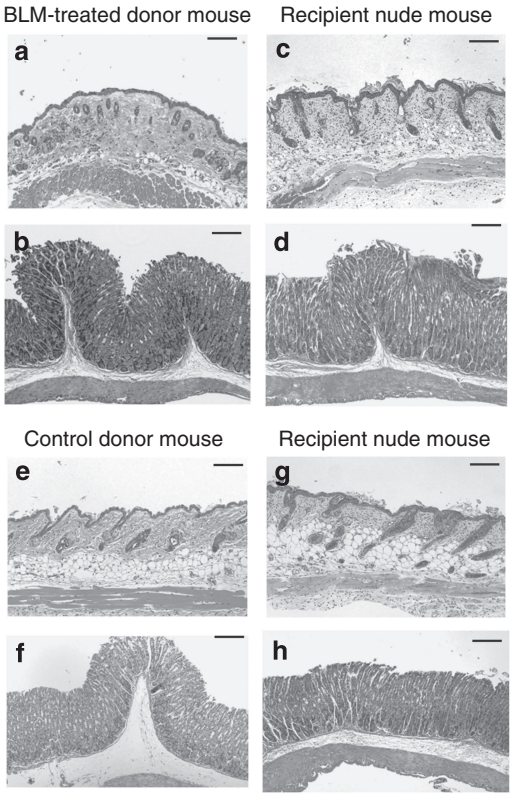

Figure 5. Reproduction of autoimmune pathology by transfer of splenocytes from BLM-treated mice. (**a**) Skin and (**b**) stomach samples taken from BLM-treated donor mouse. Dermal skin thickening and proliferation of gastric mucosa were observed. (**c**) Skin and (**d**) stomach samples taken from recipient nude mouse. Nearly the same changes were detected in these tissues. (**e**) Skin and (**f**) stomach samples taken from control mouse. No damage was seen in these tissues. (**g**) Skin and (**h**) stomach samples taken from recipient nude mouse. No tissue changes were detected. Scale bar = 100 μm. All sections stained with H&E. Representative data from three independent experiments.

$CD4^+$ T cells play a key role for tissue change and autoimmunity in this experimental model

We showed the existence of autoreactive lymphocytes in the experiments shown in Figure 5. We next asked what type of lymphocytes was essential for producing these pathological changes and autoimmunity. Thus, we compared the effects of $CD4^+$ T cells and B cells. Purification of $CD4^+$ T cells was performed as described in Materials and Methods. The purity was >90%, which was sufficient to ignore the contribution of lymphocytes other than $CD4^+$ T cells (Figure 6a). We found that the transfer of 10^6 fractionated spleen cells taken from BLM-treated mice produced nearly the same pathological changes observed with total cells (Figure 6b, c, and e). In this experiment, we also analyzed autoantibody production and observed virtually the same pattern of ANA after $CD4^+$ T cells were transferred to nude mice. The purity of B cells was also over 90% (Figure 6h–n). B cells (10^6) taken from the BLM-treated donor mouse failed to reproduce the same pathological changes (Figure 6i, j, l, and m). Although ANA was found in the donor mouse, it was not detected in the recipient mouse (Figure 6d and g). Taken together, we conclude that $CD4^+$ T cells, but not B cells in the BLM-treated mice induced the observed pathological changes and autoimmunity.

DISCUSSION

Our data indicated that continuous BLM administration induces tissue fibrosis and initiates autoimmunity. It can be noted that, we found esophageal and gastric damage related to fibrosis. Pathogenesis in our model was quite similar to SSc. Interestingly, autoantibodies, including ANAs, were also detectable. Most importantly, we verified that $CD4^+$ T cells play a central role in the induction of tissue fibrosis and autoimmunity (Figure 6). Although we used a previously published procedure to induce experimental scleroderma (Yamamoto *et al.*, 1999), to the best of our knowledge, this is the first report showing gastrointestinal involvement and suggesting a possible mechanism underlying the autoimmunity observed in this model.

In established murine models of systemic lupus erythematosus, such as MRL/lpr or NZB/W mice, genetic factors contribute to the onset of disease (Knight and Adams, 1981; Itoh *et al.*, 1994), and autoimmunity develops spontaneously. We successfully induced experimental SSc in both C3H and BALB/c mice. These findings suggest that BLM-mediated pathology is at least partially independent of genetic background. Although genetic abnormalities contribute to autoimmune diseases, environmental risk factors are also responsible (Anderson and Warner, 1976). BLM is a glycopeptide–polypeptide from *Streptomyces verticillus* that induces sequence-selective oxidative damage to nucleic

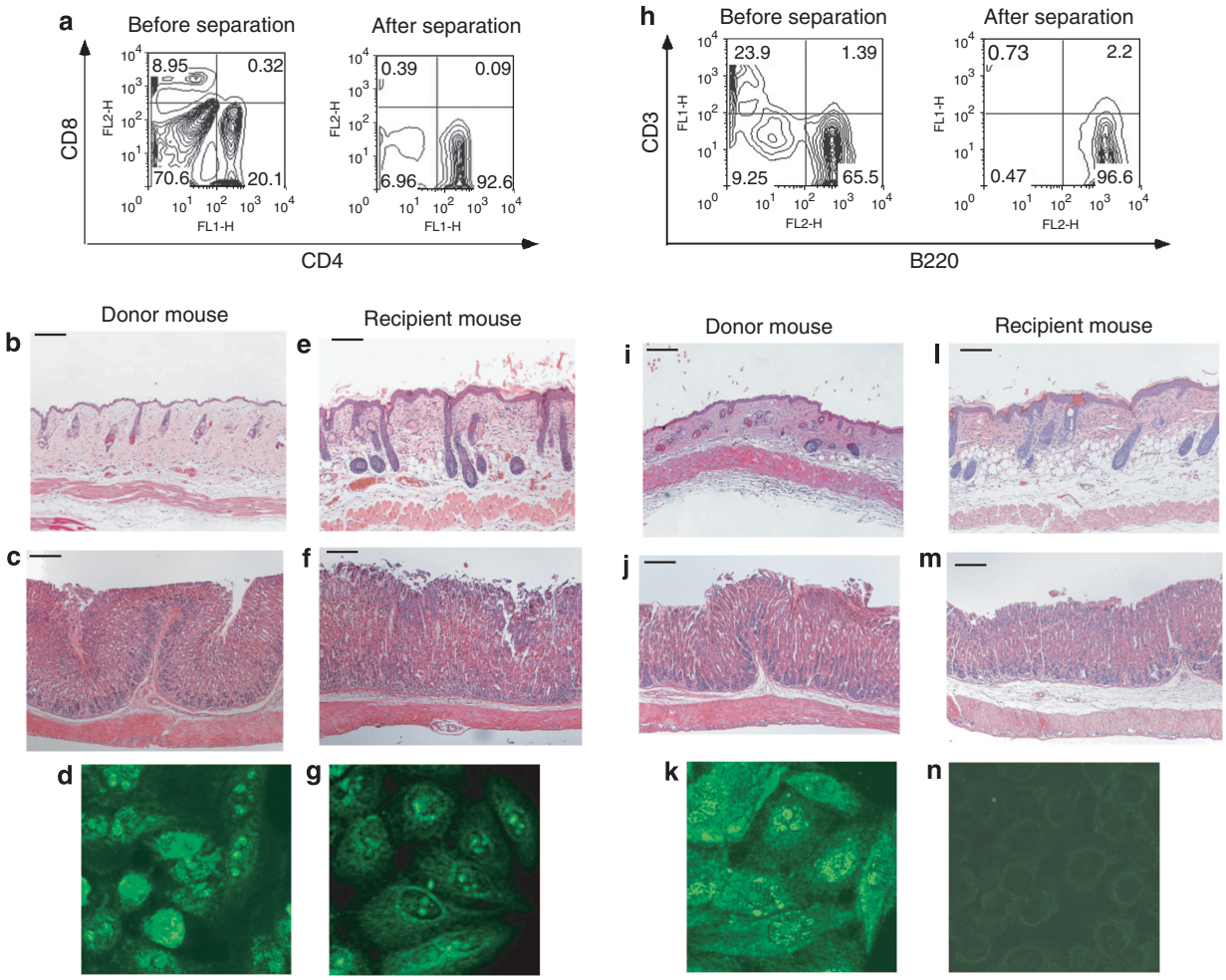

Figure 6. CD4+ T cells but not B cells play a role in the induction of pathogenesis and autoimmunity in this model. (**a**–**g**) $CD4^+$ T cells were purified by MACS as described in Materials and Methods. (**a**) Purity was >90%. (**b**, **c**) Four weeks after transfer, pathological changes were evaluated. Tissue sections from the skin and stomach were stained with H&E. (**e**, **f**) Purified $CD4^+$ cells (10^6) from BLM-treated BALB/c mice induced similar tissue damage (H&E, original magnification, ×100). The same pattern of ANA was detected in both donor mice (**d**) and recipient mice (**g**). (**h**–**n**) B cells (10^6) were also purified by MACS. (**a**) Purity was >90%. (**i**, **j**, **l**, and **m**) Despite significant pathology in the donor mouse, no tissue changes were detected in the recipient nude mouse. In addition to the pathological findings, ANA was not seen in the recipient mouse. Bars = 100 μm. Representative data from three independent experiments in panels a–n.

acids (Burger, 1998). Furthermore, oxidative stress plays a role triggering autoimmunity (Kovacic and Jacintho, 2003). Previous studies reported that an environmental factor might be involved in the etiology of SSc (Bovenzi *et al.*, 2004; Gold *et al.*, 2007). Our results support the idea that certain chemical agents may increase the risk of SSc.

Involvement of the gastrointestinal tract is the second most common manifestation of SSc. Over 80% of patients experience a change in normal gastrointestinal function (LeRoy *et al.*, 1988; Roberts *et al.*, 2006). Recent studies reported the pathogenesis of the esophagus and stomach in SSc patients (Szamosi *et al.*, 2006; Domsic *et al.*, 2008). They suggested that smooth muscle atrophy in the esophagus and fibrotic involvement of the gastric wall may account for stomach hypomotility in SSc. In our model, both the atrophic change in the esophageal wall and fibrosis of the submucosal layer of the stomach were observed. These data are consistent with the pathogenesis observed in SSc.

The presence of autoantibodies is a central feature of immune activation in SSc. SSc patients have autoantibodies that react to various intracellular components, such as DNA topoisomerase I, centromeres, RNA polymerases, U1RNP, U3RNP and Th/To, and histones (Okano, 1996). Certain Abs are characteristic of SSc, such as anti-nucleolar and anti-centromere Abs and Abs to the soluble nuclear antigen Scl-70. In our model, we confirmed the existence of specific ANAs by immunofluorescence (Figure 2). The role of autoantibodies, including ANAs in SSc, might well be important, though their significance remains unclear (Cepeda and Reveille, 2004). The relationship between the emergence of autoantibodies and fibrotic and vascular manifestations of SSc is not understood despite recent studies, suggesting that the titers of some of these autoantibodies may correlate with disease activity and clinical severity (Hu *et al.*, 2003). In our experiments, we detected autoantibodies that strongly reacted with the gastric mucosa (Figure 3). Hence, we

speculate that the production of these autoantibodies might be associated with pathogenesis in the gastrointestinal tract. The relationship between autoantibodies and pathogenesis in SSc will be analyzed in upcoming studies.

Several findings support the role of homeostatic anti-self T-cell proliferation in the pathogenesis of autoimmunity. Ionizing radiation can alter the immune system and break self-tolerance (Sakaguchi *et al.*, 1994). The exact mechanisms, which regulate the proliferation of anti-self peripheral T cells, are not fully understood. Nevertheless, evidence exists that self-MHC/peptide recognition may be seriously affected under certain conditions such as lymphopenia. We speculate that severe $CD4^+$ T-cell lymphopenia mediated by BLM is possibly the primary trigger for the autoimmune reaction in this model (Figure 4). Hence, we hypothesize that investigations focusing on the role of $CD4^+$ T cells might clarify the mechanisms of autoimmune pathology in SSc.

In our model, experimental SSc was partially reproduced by autoreactive $CD4^+$ T-cell transfer. Interestingly, B-cell transfer failed to reproduce these phenomena. Therefore, BLM-induced autoimmunity is partially mediated by activated autoreactive $CD4^+$ T cells. In donor mice, it was difficult to clearly separate the pathological changes induced directly by BLM from those by immunized lymphocytes. However, the characteristic pathological changes such as fibrosis of tissues and ANA production in recipient nude mice are mediated by ''autoreactive $CD4^+$ T cells'' derived by BLM treatment (Figures 5 and 6).

Recent studies have shown that autoreactive $CD4^+$ T cells play a key role in the induction of autoimmunity (Rankin *et al.*, 2008). The details of the mechanism are of ongoing interest. Accumulating evidence implicates cytokine networks for initiating, and either propagating or terminating fibroblast activation. Previous work investigated the possible role of Th1 and Th2 cytokines in the pathogenesis of fibrosis in an experimental animal model (Lakos *et al.*, 2006). We investigated cytokine profiles in our model and found that IL-17 release appeared to be upregulated in BLM-treated murine $CD4^+$ T cells (see Figure S2). IL-17 may be related to the induction of autoimmunity, including SSc (Stockinger *et al.*, 2007; Bettelli *et al.*, 2008; Murata *et al.*, 2008; Rueda *et al.*, 2008). Finally, there is accumulating evidence regarding the involvement of $CD4^+$ T cells in SSc (Alaibac *et al.*, 2006; Deleuran and Abraham, 2007; Parel *et al.*, 2007).

In conclusion, a mouse model of experimental SSc is not currently available. Our model possesses clinically significant features of SSc in humans and the pathology is relatively easy to induce. Our findings suggest that an environmental factor such as a chemical (BLM in this case) might be a trigger for autoimmune disease. Fibrosis and the induction of autoimmunity by autoreactive $CD4^+$ T cells in this model also merit detailed analyses. Further research with this model will fulfill an experimental need for tools to explore SSc in humans.

MATERIALS AND METHODS

Animals

Pathogen-free, female C3H/HeJ, BALB/c, and BALB/c nude mice (6 weeks old; weight about 20 g) were purchased from SLC (Shizuoka, Japan). The Animal Care and Ethics committee of Nagoya University approved the care of mice and the experimental procedures.

BLM treatment

BLM (Nippon Kayaku Co. Ltd, Tokyo, Japan) was dissolved in phosphate-buffered saline (PBS) at a concentration of 1 mg ml^{-1}. A volume of 100 µl of BLM or control PBS was injected subcutaneously with a 26-gauge needle into the shaved backs of mice 5 days per week for 3 consecutive weeks. After the final BLM or PBS injection, mice were observed without any additional treatment for an additional 3 weeks. The total experimental period was 6 weeks (42 days). There were 30–40 mice in each group (PBS or BLM). Tissue analysis and, serum and cell analyses shown in the Results section were performed the day following the final PBS or BLM treatment (on day 22) unless indicated otherwise.

Histological analyses

Tissues from the skin, lung, heart, esophagus, stomach, small intestine, liver, and spleen were removed the day following the final PBS or BLM injection (day 22). Paraffin sections were stained with either hematoxylin and eosin or MaT to evaluate histopathological changes and to detect collagen fibers in tissues. The quantitative analysis of tissues was performed as described earlier (Koca *et al.*, 2008; Liu *et al.*, 2008; Szabo *et al.*, 2008). Ice-cold, acetone-fixed cryosections (5 µm) were prepared using a cryostat (Tissue-Tek OCT, Sakura Finetec, Torrance, CA, USA) and stored at –20 °C until stained for immunohistochemistry, which was performed according to the established methods. Sections were examined using a light microscope and photographed with a digital camera (Carl Zeiss Shinjuku-ku, Tokyo, Japan).

Autoantibody detection

Tissues and cells were lysed in the sample buffer (62.5 mM Tris-HCl, pH 6.8, 2% SDS, 10% glycerol, 5% 2-mercaptoethanol, and 5% bromophenol blue). Samples (1 mg ml^{-1} total protein) were separated by electrophoresis in SDS-containing (12.5%) polyacrylamide gels and then transferred to polyvinylidene difluoride membranes (Millipore Corporation Bedford, MA). The same amount of protein was prepared for each organ. Blotted membranes were treated with 1:100 diluted serum from BLM-treated mice or control mice. The membranes were then reacted with 1:1,000 diluted horseradish peroxidase-conjugated goat IgG fraction against mouse IgG (Cappel, Durham, NC) as a secondary Ab. Detection used an enhanced chemiluminescence system (GE Healthcare Bio-Sciences Tokyo, Japan). ANAs were detected by indirect immunofluorescence methods using murine NIH3T3 cells and human Hep-2 cells (RIKEN BioResource Center, Ibaraki, Japan). Cryostat sections of control gastric mucosa were also used to detect autoantibodies. Both NIH3T3 and Hep-2 cells were grown on Chamber Slides (Lab-Tek, Nalge Nunc International, NY, USA) and fixed using −20 °C ethanol. Murine sera (diluted 1:100) from each group were incubated on the slides, followed by detection with FITC-labeled rabbit anti-mouse IgG (1:100 dilution; Invitrogen Immunodetection, San Francisco, CA, USA) according to the manufacturer's instructions. The sera from mice were stocked at −80 °C before staining.

Flow cytometry

Abs described below and reagents used in flow cytometry were purchased from eBioscience (San Diego, CA). Thymocytes and splenocytes were harvested on day 22 and stained on ice with appropriate Ab dilutions in PBS containing 0.02% sodium azide and 0.5% BSA, using FITC-conjugated anti-CD4 mAb, anti-CD3 mAb, anti-CD8 mAb, phycoerythrin (PE)-conjugated anti-CD45RB220 mAb, anti-CD8 mAb, and anti-CD4 mAb. Cells were assessed on a flow cytometer (FACS Calibur, Becton Dickinson, Tokyo, Japan), and analyzed using FlowJo software (Tomy Digital Biology, Tokyo, Japan).

Cell transfer

To determine whether autoreactive B or $CD4^+$ T lymphocytes were present in our model, and whether they induced tissue damage, splenocytes of BLM-treated BALB/c mice were injected intravenously into age-matched BALB/c nude mice. The aim of this experiment was to determine whether lymphocytes from BLM-treated mice would induce tissue fibrosis and ANA production in recipient mice. Cell donors from BLM-treated mice and PBS-treated (control) mice were killed the day after the final injection (day 22) and their spleens were removed. Spleens were placed in 6–7 ml of cold PBS/2% FBS and cut into small pieces, disaggregated by aspiration, and filtered. After three cold washes by centrifugation, the cells were resuspended in 5 ml PBS/2% FBS. Cells (10^6) were resuspended in 100 µl of PBS for injection into recipient BALB/c nude mice. For additional transfer experiments, donor mouse splenocytes were purified for B or $CD4^+$ T cells by ''negative selection.'' $CD4^+$ T cells were purified with the negative selection kit (CD4 T Cell Isolation Kit, Miltenyi-Biotec, Tokyo, Japan) using a MACS Column (LS column). For B-cell purification, we used the B Cell Isolation Kit. The magnetically labeled non-T cells or non-B cells are depleted by retention on the MACS Column (LS column) in the magnetic field of an MACS Separator, whereas the unlabeled CD4 T cells or B cells pass through the column. Finally, purified B cells or $CD4^+$ T cells (10^6) were washed three times at 4 °C and resuspended in 100 µl of PBS and then injected intravenously into recipient BALB/c nude mice. The purities of enriched B cells and $CD4^+$ T cells were evaluated by flow cytometric analysis. Representative comparisons are shown in Figure 6. Four weeks after cell transfer, skin and stomach tissues of recipient mice were taken for pathological analysis. These tissues have characteristic clinical signs of SSc for BALB/c mice. Sera of recipient mice were pooled to detect ANA. Five donors and five recipient mice of each group were used for each experiment, which was done three times (data from one representative experiment are given in the Results section).

Statistical data analysis

Results were expressed as means ± SD. Statistical data analysis was performed using StatView software (Hulinks Inc., Tokyo, Japan). Significance was determined by the Mann–Whitney *U*-test. A *P*-value <0.05 was considered significant.

CONFLICT OF INTEREST

The authors state no conflict of interest.

ACKNOWLEDGMENTS

We thank Minoru Tanaka for technical assistance with the flow cytometry. This work was supported by grants-in-aid from the Ministry of Education, Sports, and Culture of Japan and in part by grants from the Ministry of Health, Labor, and Welfare of Japan.

SUPPLEMENTARY MATERIAL

Figure S1. Immunohistochemical analysis of α-SMA.

Figure S2. Cytokine profile of the model.

REFERENCES

Abraham DJ, Varga J (2005) Scleroderma: from cell and molecular mechanisms to disease models. *Trends Immunol* 26:587–95

Alaibac M, Berti E, Chizzolini C, Fineschi S, Marzano AV, Pigozzi B *et al.* (2006) Role of cellular immunity in the pathogenesis of autoimmune skin diseases. *Clin Exp Rheumatol* 24:S14–9

Anderson RE, Warner NL (1976) Ionizing radiation and the immune response. *Adv Immunol* 24:215–335

Arnett FC, Cho M, Chatterjee S, Aguilar MB, Reveille JD, Mayes MD (2001) Familial occurrence frequencies and relative risks for systemic sclerosis (scleroderma) in three United States cohorts. *Arthritis Rheum* 44:1359–62

Bettelli E, Korn T, Oukka M, Kuchroo VK (2008) Induction and effector functions of T(H)17 cells. *Nature* 453:1051–7

Bovenzi M, Barbone F, Pisa FE, Betta A, Romeo L, Tonello A *et al.* (2004) A case-control study of occupational exposures and systemic sclerosis. *Int Arch Occup Environ Health* 77:10–6

Bowden DH (1984) Unraveling pulmonary fibrosis: the bleomycin model. *Lab Invest* 50:487–8

Burger RM (1998) Cleavage of nucleic acids by bleomycin. *Chem Rev* 98:1153–70

Cepeda EJ, Reveille JD (2004) Autoantibodies in systemic sclerosis and fibrosing syndromes: clinical indications and relevance. *Curr Opin Rheumatol* 16:723–32

Deleuran B, Abraham DJ (2007) Possible implication of the effector CD4+ T-cell subpopulation TH17 in the pathogenesis of systemic scleroderma. *Nat Clin Pract Rheumatol* 3:682–3

Domsic R, Fasanella K, Bielefeldt K (2008) Gastrointestinal manifestations of systemic sclerosis. *Dig Dis Sci* 53:1163–74

Gold LS, Ward MH, Dosemeci M, De Roos AJ (2007) Systemic autoimmune disease mortality and occupational exposures. *Arthritis Rheum* 56:3189–201

Hay J, Shahzeidi S, Laurent G (1991) Mechanisms of bleomycin-induced lung damage. *Arch Toxicol* 65:81–94

Hu PQ, Fertig N, Medsger TA Jr, Wright TM (2003) Correlation of serum anti-DNA topoisomerase I antibody levels with disease severity and activity in systemic sclerosis. *Arthritis Rheum* 48:1363–73

Itoh J, Takahashi S, Ono M, Yamamoto T, Nose M, Kyogoku M (1994) Nephritogenic antibodies in MRL/lpr lupus mice: molecular characteristics in pathological and genetic aspects. *Tohoku J Exp Med* 173:65–74

Knight JG, Adams DD (1981) Genes determining autoimmune disease in New Zealand mice. *J Clin Lab Immunol* 5:165–70

Koca SS, Isik A, Ozercan IH, Ustundag B, Evren B, Metin K (2008) Effectiveness of etanercept in bleomycin-induced experimental scleroderma. *Rheumatology (Oxford)* 47:172–5

Kovacic P, Jacintho JD (2003) Systemic lupus erythematosus and other autoimmune diseases from endogenous and exogenous agents: unifying theme of oxidative stress. *Mini Rev Med Chem* 3:568–75

Lakos G, Melichian D, Wu M, Varga J (2006) Increased bleomycin-induced skin fibrosis in mice lacking the Th1-specific transcription factor T-beta. *Pathobiology* 73:224–37

LeRoy EC, Black C, Fleischmajer R, Jablonska S, Krieg T, Medsger TA Jr *et al.* (1988) Scleroderma (systemic sclerosis): classification, subsets and pathogenesis. *J Rheumatol* 15:202–5

Liu S, Kapoor M, Shi-wen X, Kennedy L, Denton CP, Glogauer M *et al.* (2008) Role of Rac1 in a bleomycin-induced scleroderma model using fibroblast-specific Rac1-knockout mice. *Arthritis Rheum* 58:2189–95

Murata M, Fujimoto M, Matsushita T, Hamaguchi Y, Hasegawa M, Takehara K *et al.* (2008) Clinical association of serum interleukin-17 levels in systemic sclerosis: is systemic sclerosis a Th17 disease? *J Dermatol Sci* 50:240–2

Nietert PJ, Silver RM (2000) Systemic sclerosis: environmental and occupational risk factors. *Curr Opin Rheumatol* 12:520–6

Okano Y (1996) Antinuclear antibody in systemic sclerosis (scleroderma). *Rheum Dis Clin North Am* 22:709–35

Parel Y, Aurrand-Lions M, Scheja A, Dayer JM, Roosnek E, Chizzolini C (2007) Presence of CD4+CD8+ double-positive T cells with very high interleukin-4 production potential in lesional skin of patients with systemic sclerosis. *Arthritis Rheum* 56:3459–67

Povirk LF, Austin MJ (1991) Genotoxicity of bleomycin. *Mutat Res* 257:127–43

Rankin AL, Reed AJ, Oh S, Cozzo Picca C, Guay HM, Larkin J III *et al.* (2008) CD4+ T cells recognizing a single self-peptide expressed by APCs induce spontaneous autoimmune arthritis. *J Immunol* 180:833–41

Roberts CG, Hummers LK, Ravich WJ, Wigley FM, Hutchins GM (2006) A case–control study of the pathology of oesophageal disease in systemic sclerosis (scleroderma). *Gut* 55:1697–703

Rueda B, Broen J, Torres O, Simeon C, Ortega-Centeno N, Schrijvenaars MM *et al.* (2008) The interleukin 23 receptor gene does not confer risk to systemic sclerosis and is not associated with SSc disease phenotype. *Ann Rheum Dis* (in press)

Sakaguchi N, Miyai K, Sakaguchi S (1994) Ionizing radiation and autoimmunity. Induction of autoimmune disease in mice by high dose fractionated total lymphoid irradiation and its prevention by inoculating normal T cells. *J Immunol* 152:2586–95

Stockinger B, Veldhoen M, Martin B (2007) Th17 T cells: linking innate and adaptive immunity. *Semin Immunol* 19:353–61

Szabo A, Czirjak L, Sandor Z, Helyes Z, Laszlo T, Elekes K *et al.* (2008) Investigation of sensory neurogenic components in a bleomycin-induced scleroderma model using transient receptor potential vanilloid 1 receptor- and calcitonin gene-related peptide-knockout mice. *Arthritis Rheum* 58:292–301

Szamosi S, Szekanecz Z, Szucs G (2006) Gastrointestinal manifestations in Hungarian scleroderma patients. *Rheumatol Int* 26:1120–4

Tokuhashi Y, Kikkawa F, Tamakoshi K, Suganuma N, Kuzuya K, Arii Y *et al.* (1997) A randomized trial of cisplatin, vinblastine, and bleomycin versus cyclophosphamide, aclacinomycin, and cisplatin in epithelial ovarian cancer. *Oncology* 54:281–6

Varga J, Abraham D (2007) Systemic sclerosis: a prototypic multisystem fibrotic disorder. *J Clin Invest* 117:557–67

Yamamoto T (2006) The bleomycin-induced scleroderma model: what have we learned for scleroderma pathogenesis? *Arch Dermatol Res* 297:333–44

Yamamoto T, Takagawa S, Katayama I, Yamazaki K, Hamazaki Y, Shinkai H *et al.* (1999) Animal model of sclerotic skin. I: local injections of bleomycin induce sclerotic skin mimicking scleroderma. *J Invest Dermatol* 112:456–62